Journal of Materials Chemistry A

Accepted Manuscript

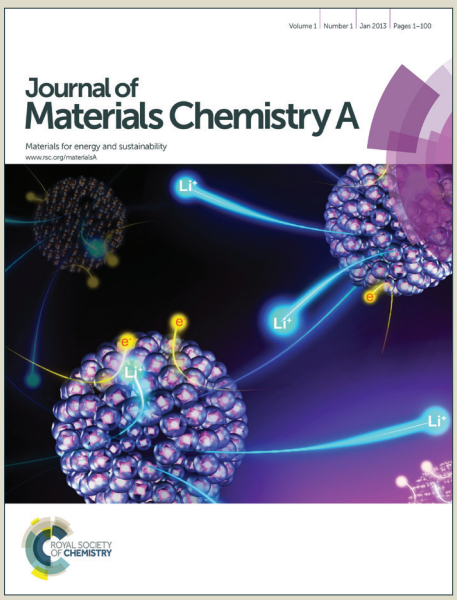

ROYAL SOCIETY OF CHEMISTRY

www.rsc.org/materialsA

Journal Name

RSCPublishing

ARTICLE

Exceptional stability of Mg-implemented PbS quantum dot solar cells realized by galvanic corrosion protection

Cite this: DOI: 10.1039/xoxxoooooox

Received ooth January 2012,
Accepted ooth January 2012

DOI: 10.1039/xoxxoooooox

www.rsc.org/

Joong Pill Park,[a] Jin hyuck Heo,[b] Sang Hyuk Im,[b]* Sang-Wook Kim[a] *

Lead sulfide (PbS) quantum dots (QDs) have been the focus of photovoltaics research because of their high quantum confinement effect and broad band absorption in the red to near-infrared (NIR) region. However, PbS QDs are easily oxidized under ambient conditions and many research groups are trying to improve their stability in air. In particular, various organic or inorganic materials are used to protect the PbS surface. In this report, we introduce the Mg-implemented PbS colloidal system (Mg–PbS) with enhanced PbS air stability. We obtained a short-circuit current density (J_{SC}) of 11.8 mA·cm^{-2}, open-circuit voltage (V_{OC}) of 0.6 V, fill factor (FF) of 62.3%, and power conversion efficiency (η) of 4.4% in a m-TiO_2 solid PV cell using Mg–PbS. In addition, their cell properties remained unchanged in a corrosive ethanedithiol solution even after 4 days because of the Mg galvanic corrosion protection of PbS QDs, whereas the PbS QD solar cells were quickly degraded by the corrosion of PbS QDs.

Introduction

Quantum dots (QDs) have been widely studied because of their unique size-dependent properties resulting from the quantum-confinement effect.[1-3] Among these properties, bandgap tunability has been a key advantage in QD applications such as light-emitting diodes (LEDs) and solar cells (SCs) because the bandgap can be precisely fitted by controlling the size without requiring the development and use of new materials. In particular, lead sulfide (PbS) QDs have garnered great interest owing to their small bulk bandgap of ~0.41 eV and long exciton Bohr radius of 18 nm, which enable their application in the near-IR (NIR) segment of the solar spectrum.[4-6] In solar cell applications in particular, 50% of the photons are in the NIR range below 1.8 eV, which highlights the importance of PbS QDs as an absorber. The light absorption of PbS QDs can be controlled in a wide spectral region, specifically from red to NIR, through strong quantum confinement. In addition, PbS QDs are known to be a good example of material for demonstrating ground-breaking SCs by exploiting multiple exciton generation (MEG); currently, their efficiency reached over 7% at 1 sun (100 mW·cm^{-2} AM 1.5 G). Although PbS QDs have great potential for application in SCs, they have inherent drawbacks such as poor stability in air resulting from oxidation because the binding energy of Pb–O (378 kJ·mol^{-1}) is stronger than those of other metals such as Zn–O (284 kJ·mol^{-1}) and Cd–O (142 kJ·mol^{-1}). Therefore, it is necessary to develop stable PbS QDs before they can be successfully applied to SCs.

To overcome the stability issue, core–shell structured QDs[7,8] have been developed. Compared to QDs without shells, core–shell structured QDs are known to exhibit significantly improved stability, quantum yield (QY), and optical properties. From a material synthesis perspective, however, core–shell structured QDs are only formed when they meet specific conditions, namely, when the core and shell have the same crystal structure and similar lattice parameters. For instance, since CdSe and ZnSe have the same zinc-blend crystal structure and small lattice mismatch of 6.3%,[9] they can form the core–shell CdSe–ZnSe structure. It is known that QDs based on CdE (E: S, Se, Te) and InX (X: P, As) can form the core–shell structure because they have similar zinc-blend or Wurtzite structure and small lattice mismatch.[7] However, it is difficult to find a proper shell candidate for PbS QDs because they have a distinct rock-salt crystal structure and a large lattice parameter of 5.9 Å. The PbS–PbSe core–shell- and PbS–PbSe alloy-structured QDs have been reported because PbSe has a structure similar to that of PbS and a small lattice mismatch.[10-12] Recently, new heterostructured QDs such as PbS–CdS and PbS–CdSe have been formed by the cation-exchange method,[13-16] but the type-I core–shell-structured QDs are not adequate for SCs because they cannot efficiently transfer or transport charge carriers owing to the quantum-well structure.[17,18]

To improve the stability of PbS QDs while preserving the SC performance, it is desirable to i) form a more stable molecular or atomic shell than PbS or ii) supplement PbS with oxygen or a corrosion-scavenging element. The former has been demonstrated by using a –SH molecular shell such as ethanedithiol (EDT) and dodecanethiol (DDT),[21,22] or a halide[23] atomic shell. However, even though the device efficiency can be greatly improved, the –SH molecular shells tend to be oxidized or detached from the PbS QDs. The halide atomic ligands are also known to improve the device efficiency and stability,[24] but their synthesis seems to be tricky. Consequently, the second approach seems to offer more benefits because it improves the stability of PbS itself and provides more room to independently control the surface of PbS QDs. We implemented PbS QDs with Mg as a galvanic corrosion-protection element because Mg is generally used as a galvanic sacrificial material to protect base metals such as steel and lead with higher anodic index. Compared with Pb, Mg has a relatively low reduction potential and high oxygen affinity so that oxygen molecules adhere to Mg first and the surface Pb ions will be protected as a result. In the study reported here, we synthesized the Mg-implemented PbS QDs by hot solution chemistry and examined the stability of Mg-implemented PbS QDs and SCs.

Results and discussion

Optical properties and crystal structure of Mg–PbS

The synthesized Mg–PbS was analyzed using inductively coupled plasma atomic emission spectroscopy (ICP-AES), transmission electron microscopy (TEM), X-ray diffraction (XRD), and absorption spectroscopy. ICP elemental analysis showed a maximum Mg concentration of 1.5% despite the increase in the input amount of magnesium acetate tetrahydrate (ESI, Figure S1).

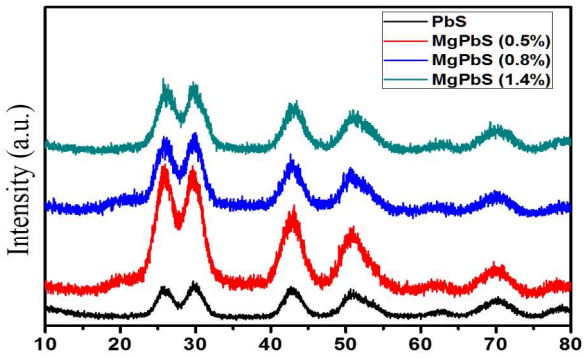

Figure 1. XRD pattern of various Mg-PbS QDs.

Figure 1 shows the powder XRD patterns of PbS and three different Mg–PbS samples. There were no changes to the peaks or shifts in the patterns of the Mg–PbS samples from that displayed by PbS, indicating that the rock-salt crystal structure of PbS was stably maintained despite the addition of Mg. We measured the sizes of three different Mg–PbS QDs using the TEM images (Figure 2a), revealing that they were similar in size (~3 nm) and non-spherical in shape. More detailed TEM images are provided in ESI (Figure S2). We intentionally targeted synthesis of PbS QDs with the specific size of 3 nm because the resultant 1000 nm absorption is suitable for solar cell applications.

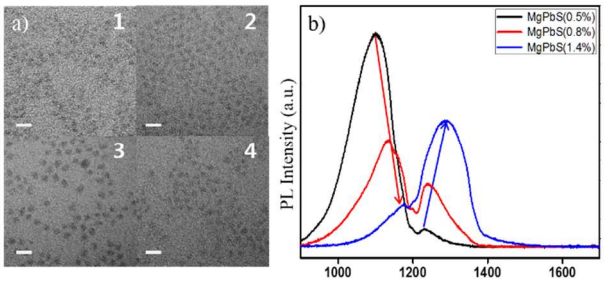

Figure 2. TEM image of PbS QDs which have various Mg contents. PbS (a-1) 0.5 % Mg-PbS (a-2), 0.8 % Mg-PbS (a-3), and 1.4 %Mg-PbS (a-4) (Scale bar: 5nm). And PL spectrum of magnesium implemented PbS QDs.

The optical properties of PbS and Mg–PbS QDs were studied using absorption and photoluminescence (PL) spectroscopy. The band-edge absorption peaks of one PbS and three different Mg–PbS QDs showed small red shifts from 930 to 962 and 1084 nm as the amount of Mg increased (Figure 3). In additional, the PL spectra showed interesting results (Figure 2b). Two peaks representing a red-shifted band-edge emission and a surface-trap emission were observed in the spectra of Mg–PbS QDs. The red-shifted absorption and emission resulted from a change in the band alignment caused by the Mg-implemented surface. A similar change in the band offset caused by the surface modification was reported by other research groups.[19,20]

When the amount of Mg increased, the PL peak corresponding to the surface-trap emission also increased. The PL peak of the band-edge emission decreased under the same circumstances. Based on these results, we assume that the Mg ion of Mg–PbS was located on the surface of the PbS QD and acted as a surface defect. The experimental data suggest that the Mg-implementing process might have had a negative effect on the PbS properties. However, as discussed below, stability tests revealed an unexpected outcome.

PbS-material-stability test

Air-stability tests were performed on both the pure PbS QD and three Mg–PbS QDs. Every sample was dispersed in hexane and kept under ambient conditions. Absorption of all samples was measured to assess the state of surface oxidation every 5 days. The excitonic absorption peak of the pure PbS QD gradually shifted from 1022 to 1004 nm over 50 days (Figure 3a). We controlled the ratio of the Pb precursor to S precursor to induce Pb-rich facets,[26,27] which led to more stable surfaces because of the increase in ligand (OA) binding to the Pb surface.

In comparison, Mg–PbS QDs showed various results as the amount of Mg changed (Figure 3b–d). Three Mg–PbS samples containing 0.5, 0.8, and 1.4% of Mg showed absorption-peak blue-shifts of 10, 16, and 24 nm, respectively, over 50 days. The 0.5%Mg–PbS QD with a 10-nm shift showed improved absorption compared to the pure PbS QD; however, the stability in air decreased as the amount of Mg increased. The peak shift was mainly caused by the oxidation of Pb at the surface.[19,20] The reduction potentials of Pb and Mg are −0.13 and −2.37 eV, respectively, which means that it is easier to oxidize Mg. The binding energy between Mg and O (394 kJ·mol^{-1}) is also larger

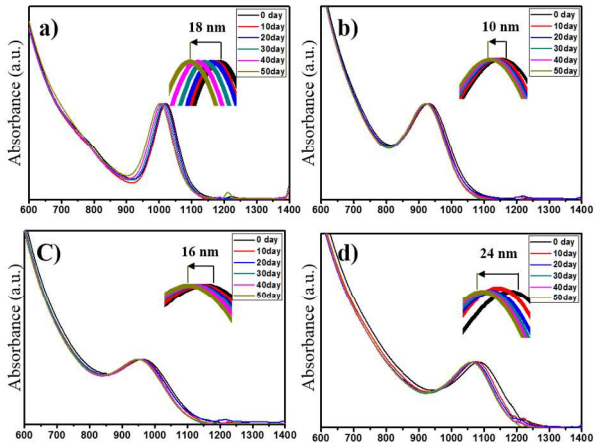

Figure 3. UV absorbance spectrums changes over 50 days of PbS QDs in ambient conditions which have various Mg ion contents. 0 % (a), 0.5 % (b), 0.8 % (c), and 1.5% (d).

than that between Pb and O (378 kJ·mol^{-1}). Thus, the presence of Mg on the PbS QD surface protected the Pb surface from oxidation by undergoing oxidation before Pb had the chance to be oxidized.

We measured the binding energy of the 4f^7 state of Pb and 1s state of O1s using X-ray photoelectron spectroscopy (XPS) to confirm that surface oxidation occurred (Figure 4). Each QD sample was released in droplets on a washed glass surface and stored in a convection oven (120 °C) for 1.5 h for the high temperature to accelerate surface oxidation. In the 4f^7 Pb spectra, the peaks at 136.8 and 137.9 eV indicate the presence of PbS and PbO, respectively,[28,29] implying that Pb located on the surface of the PbS QDs was partially oxidized. The spectrum of pure PbS shows both peaks while the Mg–PbS spectrum shows only one peak with an energy of 137.1 eV, revealing that Mg protected the PbS surface and prevented surface oxidation.

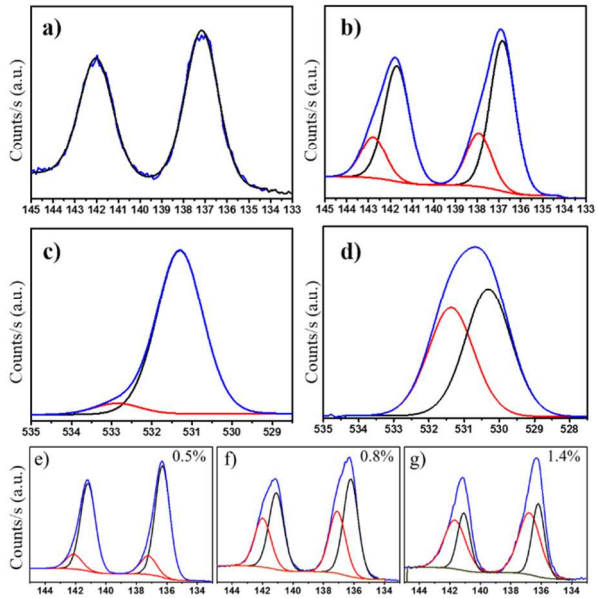

Figure 4. Pb 4f XPS spectrums of Mg-PbS (a) and PbS (b), O 1s XPS spectrum of Mg-PbS (c) and PbS (d). Pb 4f XPS spectrum of Mg-PbS with various Mg contents (e, f, g)

In the spectra of the 1s orbitals of O, the peaks at 530.3 and 531.4 eV indicate the presence of PbO and Pb oleate, respectively.[28,29] A peak with an energy of 531.4 eV was observed in the spectra of pure PbS and Mg–PbS, implying that it originated from surface binding between Pb and OA. This was confirmed by the XPS measurement of as-synthesized Pb oleate (ESI Figure S3).

The lack of a peak at 530.4 eV in the spectrum of the Mg–PbS QDs shows the restriction of Pb oxidation at the surface. A small peak at 532.9 eV in the O1s spectrum of Mg–PbS originated from MgO, and the high binding energy compared to PbO originated from the high Mg charge density. We also performed XPS measurements using three Mg–PbS samples containing 0.5, 0.8, and 1.4% of Mg. (Fig. 4e, 4f, and 4g) Pb-O peaks in high energy region (red color) are gradually increased compared with Pb-S (black color) as Mg contents is increase. The data reveals that a large amount of Mg leads oxidation of QD surface and this result is matched up with absorbance data shown in Fig. 3.

Although we have not determined why greater amounts of Mg aggravated PbS QD stability, we speculate that the ease of oxidation of Mg complicated the situation.

Mg–PbS QD sensitized solar cells

To check if the colloidal Mg–PbS QD sensitized solar cells were still exceptionally stable, we fabricated solar cells composed of F-doped tin oxide (FTO), dense blocking TiO_2 (approximately 50-nm-thick), mesoporous TiO_2 (approximately 500-nm-thick), Mg–PbS QDs, and Au, as shown in Figure 5(a). Upon illumination, the Mg–PbS QDs absorbed the light and generated electron–hole pairs. The generated electrons and holes were then transported into the mesoporous TiO_2 electron conductor and Au counter electrode, respectively.

Figure 5(c) shows the J–V curves of Mg–PbS QD solar cells, which exhibited J_{SC} of 11.8 mA·cm^{-2}, V_{OC} of 0.6 V, FF of 62.3%, and η of 4.4% under standard solar conditions (100

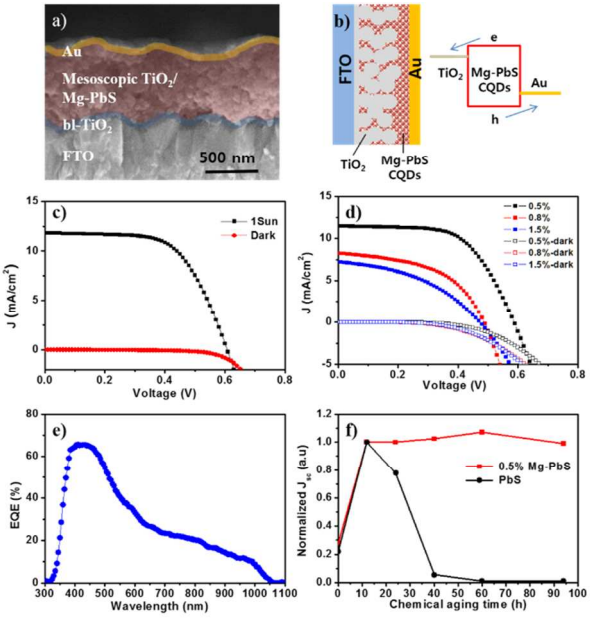

Figure 5. SEM cross section image (a), illustration of cell (b), J-V curve measurement of best cell performance with 0.5% Mg (c), J-V curve of Mg-PbS cell with various Mg contents (d), EQE spectrum of cell with 0.5% Mg (e) and cell stability test under ambient condition (f).

mW·cm^{-2} AM 1.5G). The high efficiency of Mg–PbS QD sensitized solar cells are attributed to the relatively higher V_{OC} and FF compared to conventional PbS QD solar cells owing to the reduced oxidation of PbS QDs via the implement of Mg. The value of J_{SC} (12 mA·cm^{-2}) calculated by integrating the external quantum efficiency (EQE) spectrum, as shown in Figure 5(e), is consistent with J_{SC} of Mg–PbS QD solar cells. As a comparison data, solar cell using 0% (bare PbS), 0.8% and 1.5 % Mg-PbS were also fabricated and their cell properties were measured. (Fig. 5d) The data shows that 0.5% Mg-PbS are optimized QD system for solar cell application.

In our previous study, we found that a post-synthesis 1,2-EDT treatment improved device efficiency because the replacement of long OA ligands with short EDT ligands improved the interfacial contact between PbS QDs. However, PbS QDs were quickly degraded or oxidized after treatment and color fading occurred. Therefore, we treated PbS QD and Mg–PbS QD solar cells in an anhydrous ethanol solution with 5 wt% EDT, as shown in Figure 5(f). The Mg–PbS QD solar cells did not show a significant degradation in η with increasing EDT-treatment duration, whereas the PbS QD device quickly degraded as the treatment duration was increased. The exceptional stability of Mg–PbS QD solar cells is attributed to the greatly enhanced stability of Mg–PbS QDs in air resulting from the incorporation of Mg, which acted as a sacrificial oxygen scavenger through its higher oxidation probability compared to Pb.

Experimental

Lead(II) acetate trihydrate ($Pb(Ac)_2{\cdot}3H_2O$; 99.999% metal basis, Aldrich), magnesium acetate tetrahydrate ($Mg(Ac)_2{\cdot}4H_2O$; 99%, Aldrich), oleic acid (OA; 90%, Aldrich), 1-octadecene (ODE; 99%, Aldrich), and bis(trimethylsilyl)sulfide (TMS-S; 95%, Acros) were used as purchased without further purification.

Colloidal PbS QDs were synthesized according to the methodology reported by Jeong et al.[27] To prepare 0.5%Mg–PbS QDs, 0.625 mmol (237 mg) of $Pb(Ac)_2{\cdot}3H_2O$, 0.625 mmol (134 mg) of $Mg(Ac)_2{\cdot}4H_2O$, 1.6 mL of OA, and 8 mL of ODE were mixed in a 50-mL three-neck flask. The mixed solution was degassed under vacuum at 60 ºC for 0.5 h, after which it was heated to 110 ºC and kept at that temperature for 1 h. The flask was then recharged with nitrogen. The precursor solution was prepared by adding 0.05 mL of TMS-S to 1 mL of ODE. When the temperature of the flask reached 95 °C, the precursor solution was rapidly injected into the mixed solution and the heating mantle was removed. The color of the reaction solution changed from colorless to dark red. The solution was maintained at 60 °C for 1 h. Finally, PbS QDs were isolated from the mixture by adding 40 mL of ethanol, followed by two or three cycles of centrifugation at 3500 rpm for 5 min.

Conclusions

We introduced the Mg-implemented PbS colloidal system (Mg–PbS) to enhance the QD stability in air and their SC properties. The idea is based on the relatively low reduction potential and high oxygen affinity of Mg. We investigated the optimal contents of Mg and 0.5% Mg-PbS show the best air stability and cell performance. We obtained a short-circuit current density (J_{SC}) of 11.8 mA·cm^{-2}, open-circuit voltage (V_{OC}) of 0.6 V, fill factor (FF) of 62.3%, and power conversion efficiency (η) of 4.4% in a m-TiO_2 solid PV cell using Mg–PbS. In addition, their cell properties were preserved in the corrosive 1,2-ethanedithiol solution even after 4 days owing to the presence of Mg in Mg–PbS QDs, whereas the PbS QD solar cells were quickly degraded by the corrosion of PbS QDs within 2 days.

Acknowledgements

This work was supported by the New & Renewable Energy Core Technology Program of Korea Institute of Energy Technology Evaluation and Planning (KETEP) (No. 201330300001) and the Basic Science Research Program through the National Research Foundation of Korea (NRF) funded by the Ministry of Science, ICT & Future Planning (No. 2014R1A5A1009799), Republic of Korea.

Notes and references

[a] Department of Molecular Science and Technology, Ajou University, Suwon 443-749, Korea.
[b] Functional Crystallization Center, Department of Chemical Engineering, Kyung Hee University 1732 Deogyoung-daero, Giheung-gu, Yongin-si, Gyeonggi-do 446-701, Republic of Korea.

1 G. D. Scholes, *Adv. Funct. Mater*, 2008, **18**, 1157-1172.
2 M. A. Hines, G. D. Scholes, *Adv. Mater*, 2003, **15**, 1844-1849.
3 D. J. Norris, A. Sacra, C. B. Murray, M. G. Bawendi, *J phys. Rev. Lett.*1994, **72**, 2612-2615.
4 G. D. Scholes, G. Rumbles, *Nat. Mater*, 2006, **5**, 683-696.
5 A. Guchhait, A. K. Rath, A. J. Pal, *Appl Phys Lett*, 2010, **96**, 073505.
6 J. Seo, S. J. Kim, W. J. Kim, R. Singh, M. Samoc, A. N. Cartwright, P. N. Prasad, *Nanotechnology*, 2009, **20**, 095202.
7 P. Reiss, M. Protie`re, L. Liang, *small*, 2009, **5**, 154-168.
8 M. A. Hines, P. G. Sionnest, *J. Phys. Chem*, 1996, **100**, 468-471.
9 X. Peng, M. C. Schlamp, A. V Kadavanich, A. P. Alivisatos, *J. Am. Chem. Soc*, 1997, **119**, 7019-7029.
10 W. Ma, J. M. Luther, H. Zheng, Y. Wu, A. P. Alivisatos, *Nano. Lett*, 2009, **9**, 1699-1703.
11 H. Wang, J. Wang, X. Caoc, G. J. Snyder, *J. Mater. Chem. A*, 2014, **2**, 3169-3174
12 A. C. Bartnik, F. W. Wise, *phys. Rev. Lett.B*, 2007, **75**, 245424;
13 H. Zhao, M. Chaker, N. Wub, D. Ma, *J. Mater. Chem*, 2011, **21**, 8898-8904.
14 B. Mukherjee, A. Peterson, V. Subramanian, *Chem. Commun*, 2012, **48**, 2415-2417.
15 F. Ren, H. Zhao, F. Vetrone, D. Ma, *Nanoscale*, 2013, **5**, 7800-7804.
16 K. A. Abel, P. A. FitzGerald, T. -Y. Wang, T. Z. Regier, M. Raudsepp, S. P. Ringer, G. G. Warr, F. C. J. M. van Veggel, *J. Phys. Chem. C*, 2012, **116**, 3968-3978.
17 H. Zhao, H. Liang, B. A. Gonfa, M. Chaker, T. Ozaki, P. Tijssen, F. Vidala, D. Ma, *Nanoscale*, 2014, 6, 215-225.
18 J. B. Sambur, B. A. Parkinson, *J. Am. Chem. Soc,* 2010, **132**, 2130-2131.
19 J. F. Peterson, T. D. Krauss, *Phys. Chem. Chem. Phys,* 2006, **8**, 3851-3856.

20 Y. Zhang, J. He, P. -N. Wang, J. -Y. Chen, Z. -J. Lu, D. -R. Lu, J. Guo, C. -C. Wang, W-L. Yang, *J. Am. Chem. Soc*, 2006, **128**, 13396-13401.
21 R. Ihly, J. Tolentino, Y. Liu, M. Gibbs, M. Law, *ACSnano*, 2011, **5**, 8175-8186.
22 S. Kim, S. H. Im, M. Kang, J. H. Heo, S. I. Seok, S. -W. Kim, I. Mora-Sero, J. Bisquertc, *Phys. Chem. Chem,* 2012, **14**, 14999-15002.
23 J. Zhang, J. Gao, E. M. Miller, J. M. Luther, M. C. Beard, *ACS Nano*, 2014, **8**, 614-622.
24 C. M. Chuang, P. R. Brown, V. Bulovic, M. G. Bawendi, *Nat. Mater*, 2014, **13**, 796-801
25 J. Tang, X. Wang, L. Brzozowski, D. A. R. Barkhouse, R. Debnath, L. Levina, E. H. Sargent, *Adv. Mater*, 2010, **22**, 1398-1402.
26 M. C. Weidman, M. E. Beck, R. S. Hoffman, F. Prins, W. A. Tisdale, *ACS Nano*, 2014, **8**, 6363-6371.
27 H. Choi, J. -H. Ko, Y. -H. Kim, S. Jeong, *J. Am. Chem. Soc*, 2013, **135**, 5278-5281.
28 E. Godocikova, Z. Bastl, I. Spirovova, P. Balaz, *J. Mat. Sci,* 2004, **39**, 3025-3029.
29 J. D. Patel, F. Mighri, A. Ajji, S. Elkoun, *MSA,* 2012, **3**, 125-130.

Table of Contents

Mg-implemented PbS colloidal system enhance the QD stability in air and their solar cell stability after EDT treatment.

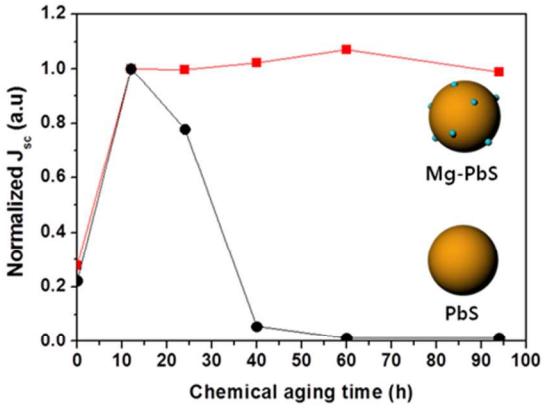

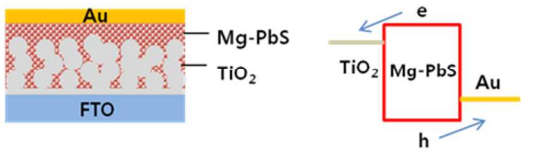

	Voc (V)	Jsc (mA/cm2)	F.F. (%)	η (%)
Mg-PbS	0.6 → 0.6	11.8 → 12	62.3 → 61.7	4.4 → 4.37
PbS	0.47 → 0.42	12.4 → 0.29	38.8 → 50.2	2.2 → 0.06